J Mater Sci (2020) 55:1904–1914

Ceramics

Preparation and characterization of $(Ba_{0.85}Ca_{0.15})(Zr_{0.1}Ti_{0.9})TiO_3$(BCZT)/$Bi_2O_3$ composites as efficient visible-light-responsive photocatalysts

S. Abhinay[1], P. Tarai[1], and R. Mazumder[1,*]

[1] *Department of Ceramic Engineering, National Institute of Technology, Rourkela, Odisha 769008, India*

Received: 14 August 2019
Accepted: 30 October 2019
Published online: 7 November 2019

ABSTRACT

The heterojunction composites $(Ba_{0.85}Ca_{0.15})(Zr_{0.1}Ti_{0.9})TiO_3$(BCZT)/$Bi_2O_3$ with different weight ratios (75:25, 50:50 and 25:75) were successfully synthesized by solid-state route. As-synthesized composite powders were characterized by XRD, FESEM, EDX, UV–visible and photoluminescence spectroscopy. Photocatalytic activity evaluation was carried out by the degradation of rhodamine B (RhB) under UV and visible light exposure. The results show that the heterojunction composites BCZT/Bi_2O_3 display better photocatalytic activity than pure BCZT or Bi_2O_3. Among all the heterojunction composites, BCZT/Bi_2O_3 (50:50) composite exhibits a lower recombination rate of electron–hole pair and shows the highest photocatalytic activity. The rate constant of BCZT/Bi_2O_3 (50:50) composite for RhB degradation is 15.4 and 2.1 times higher than those of pure BCZT and Bi_2O_3 under visible light irradiation, respectively. Finally, a possible mechanism for enhanced charge separation and photodegradation is proposed.

Introduction

Contamination of the water bodies is one of the major global problems, thus affecting the equilibrium of ecosystem which is caused by dumping all the waste from textile industries, chemical industries and other harmful organic pollutants due to rapid industrialization. There are many ways to treat these wastes such as filtration, ion exchange, biological treatment and adsorption on activated charcoal, but they have disadvantages such as high cost, low efficiency and high sludge production. Photocatalytic oxidation process has been extensively studied owing to its advantages such as low cost, non-toxic, stability under illumination and high reproducibility. Since the past decades, many semiconductor systems such as TiO_2 [1], ZnO [2] and SnO_2 [3] had been studied for photocatalytic activity. But the problems with this system are that they can utilize only 4% (UV) of the solar spectrum and high recombination rate of electrons and holes. There are many strategies to tackle this problem such as introduction of defect levels into the band gap by doping, metallization and heterojunction formation. Among all these strategies,

Address correspondence to E-mail: rana_brata@hotmail.com

https://doi.org/10.1007/s10853-019-04175-3

heterojunction coupling of two or more semiconductors has been the most effective strategy to enhance the lifetime of electrons and holes, owing to its advantages including non-toxicity, non-selectivity, cost-effectiveness and total removal of pollutants [4].

Ferroelectric oxides such as PZT [3, 5, 6], $BaTiO_3$ [7–10], $KNbO_3$ [11] and $SrTiO_3$ [12] are also studied for photocatalytic applications. But the problem with these systems is that they have high band gap (> 3 eV), thus utilizing only UV portion of solar spectrum. The advantage of these systems is the presence of inbuilt electric filed which helps in separation of electrons and holes, thus enhancing their life span [13–15]. In order to enhance the photoabsorption in visible region of solar spectrum, heterojunction has been made with Bi_2O_3 [16–19], Cu_2O [20], Ag_2O [21] and Fe_2O_3 [22] due to their matching band potentials with ferroelectric systems. Among different narrowband gap oxides (Bi_2O_3, Cu_2O, Ag_2O and Fe_2O_3) semiconductors, Bi_2O_3 is preferred due to having a band gap of 2.2 eV, strong oxidation ability of the valence band (VB) and excellent visible-light-absorbing capacity. Despite the advantages of Bi_2O_3, it is seldom used as a photocatalyst due to the reduction capability of conduction band (CB) (0.63 eV) which is more positive than the potential of $O_2/{}^*O_2^-$ (− 0.33 eV). Therefore, the e^- on the CB of Bi_2O_3 cannot reduce the adsorbed O_2 into ${}^*O_2^-$, which results in short life span of charge carriers [23]. During the past few years, many reports are available on the preparation of oxide ferroelectrics–narrowband gap oxide heterostructure due to polarization-dependent surface properties of heterogeneous photocatalyst. Among them, PZT/TiO_2 [6], $Bi_2O_3/BaTiO_3$ [17, 19], $Fe_2O_3/BaTiO_3$ [22] and $Bi_2O_3/KNbO_3$ [18] have been promising. The breakthrough made by Liu and Ren et al. in $BaTiO_3$ ceramics with Ca and Zr co-doping [$0.5Ba(Zr_{0.2}Ti_{0.8})O_3$–$0.5(Ba_{0.7}Ca_{0.3})TiO_3$] has offered a significant impact on the development of lead-free piezoceramics. The high saturation polarization ($17\mu C/cm^2$) and large piezoelectric properties ($d_{33} > 500pC/N$) of BCZT make it a potential material for ferroelectric and piezoelectric applications [24–26]. However, BCZT is a wide band gap material. The fabrication of heterojunction with narrow band gap oxide semiconductor with matching band potentials can facilitate the high visible light activity and interfacial charge transfers and enhance the life span of photoinduced charge carriers. Till now, to the best of our knowledge there is no literature available on photocatalysis of BCZT and there are also no reports available on formation of heterojunction with BCZT. The present paper aims to improve the photocatalytic activity of BCZT by making heterojunction with Bi_2O_3. So, in the present work heterojunction has been made between BCZT and Bi_2O_3 which has a band gap of 2.2 eV and matching band potentials. In the present work, the objective is to make the heterojunction between BCZT and Bi_2O_3 by varying weight ratios and to study the effect of composite on UV–visible absorption spectrum and photocatalysis. Finally, a mechanism behind the photocatalytic degradation of RhB has also been proposed.

Experimental procedure

Synthesis of BCZT

BCZT was synthesized by conventional solid-state reaction route. Barium carbonate (Sigma-Aldrich, 99%), calcium carbonate (Sigma-Aldrich, 99%), zirconium dioxide (Sigma-Aldrich, 99.9%) and titanium dioxide (Sigma-Aldrich, 99.0%) were used as precursor materials. A stoichiometric amount of powders was mixed by a planetary mill (Fritsch Pulverizer) for 10 h with zirconia ball using isopropyl alcohol as the media. The mixture was dried at 100 °C overnight in an oven. The mixture was placed in an alumina crucible, which was subsequently inserted into the furnace and calcined at 1300 °C/4 h, in air.

Fabrication of BCZT/Bi_2O_3 composite

$BCZT/Bi_2O_3$ composite was prepared by solid-state method. Nano-Bi_2O_3 (Sigma-Aldrich, 99%) and the prepared BCZT were weighed according to BCZT: Bi_2O_3 = 100:0%, 75:25%, 50:50%, 25:75% and 0:100% (mass ratio). After that the powders were wet milled in pot mill using isopropanol for 6 h. The mixture was dried under IR lamp and calcined at 500 °C for 1 h. The reason for calcination is to provide sufficient bonding between the two oxides, which could provide a special condition for charge transfer from one particle to another via interfaces.

Characterizations

XRD patterns of the composites were recorded by Rigaku Ultima-IV with CuKα (1.54178A°). The particle morphology was characterized by using FESEM [Nova NanoSEM 450] and TEM (Tecnai G230ST-FEI). Photoluminescence analysis was obtained by using a WITec alpha 300R, using an excitation wavelength of 355 nm. The light absorption spectrums were measured using a UV–visible spectrophotometer (PerkinElmer, USA) equipped with an integration sphere. The photocatalytic reaction was carried out in a stirred photoreactor with a capacity of 400 mL with a medium-pressure mercury vapor lamp 250 W and high-pressure mercury vapor lamp 450 W (Lelesil) placed inside the photoreactor as the main UV and visible irradiation sources. The inner immersion well was fixed with a water inlet and outlet for cold water circulation during the photochemical process. For photocatalytic experiments, initially 100 mg of the sample was added to 100 ml of rhodamine B (RhB) solution (10 mg/L) and ultrasonicated for 5 min. Initial pH of the RhB solution was ~ 5. Later, the mixture was stirred in the dark condition for 30 min to reach the adsorption/desorption state of equilibrium. Periodically (15 min), a 10-ml sample was injected out of the reaction vessel and the extent of degradation was measured by using Eq. (1).

$$\text{Degradation}\,(\%) = \left(1 - \frac{C}{C_0}\right) * 100 \qquad (1)$$

where C_0 is the concentration at time 't_0' and C is the concentration at time 't'.

Experiments were also carried out under different pH conditions (1, 3, 9 and 11). pH of the RhB solution was varied by adding HCl or 1 M NaOH solutions. Finally, to check the reusability, the photocatalyst was separated by centrifugation after each cycle and used for the next cycle without any pre-treatment.

Results and discussion

XRD analysis

Figure 1 shows the XRD patterns of BCZT, Bi_2O_3 and BCZT/Bi_2O_3 composites with different weight ratios synthesized by solid-state route. For pure BCZT, all the diffraction peaks can be assigned to the tetragonal phase (JCPDS File No. 89-1428) and pure Bi_2O_3 was monoclinic (JCPDS File No. 71-2274). In the case of BCZT/Bi_2O_3 composite, there were two sets of diffraction peaks, which were correspondingly ascribed to tetragonal BCZT and monoclinic Bi_2O_3. No other characteristic peaks were detected, indicating that as-prepared composites consist of tetragonal BCZT and monoclinic Bi_2O_3 and no appreciable chemical reaction occurred between BCZT and Bi_2O_3 during the calcination process at 500 °C.

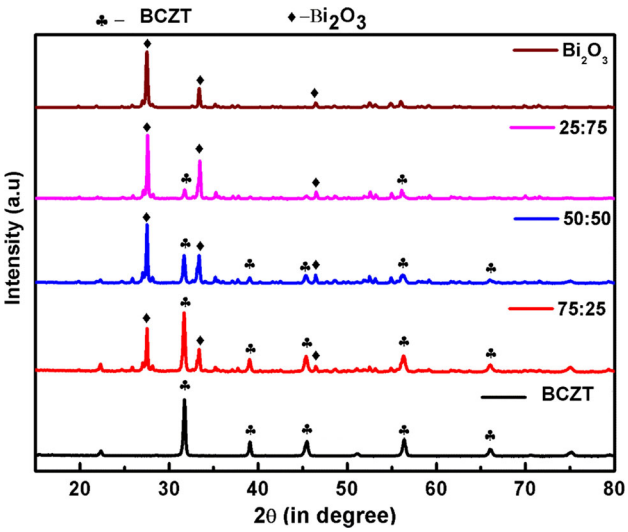

Figure 1 XRD patterns of the as-prepared samples with different BCZT/Bi_2O_3 mass ratios prepared by solid-state route.

UV–visible spectroscopy

The UV–visible absorption spectra of prepared composites by solid-state method are shown in Fig. 2. The band gap of BCZT and Bi_2O_3 was found to be 3.1 eV and 2.2 eV, respectively. The optical absorption of BCZT/Bi_2O_3 composite prepared by solid-state route starts at about 550 nm. With increasing Bi_2O_3 content, absorbance intensity of composite increases under visible light. It can be observed that BCZT/Bi_2O_3 heterostructures show broad absorption bands, which shows that the composites have enhanced visible light absorption when compared with pure BCZT. In the present study, two absorption edges can be clearly observed when the content of Bi_2O_3 reaches 75% and 50% for the samples prepared by this synthesis technique. Xi et al. [17] reported that two absorption edges can be found when the content of Bi_2O_3 reaches 90%, and according to Fan et al. [19], single absorption edge can be observed for 75:25 and 50:50 Bi_2O_3/$BaTiO_3$ composite. So BCZT/Bi_2O_3

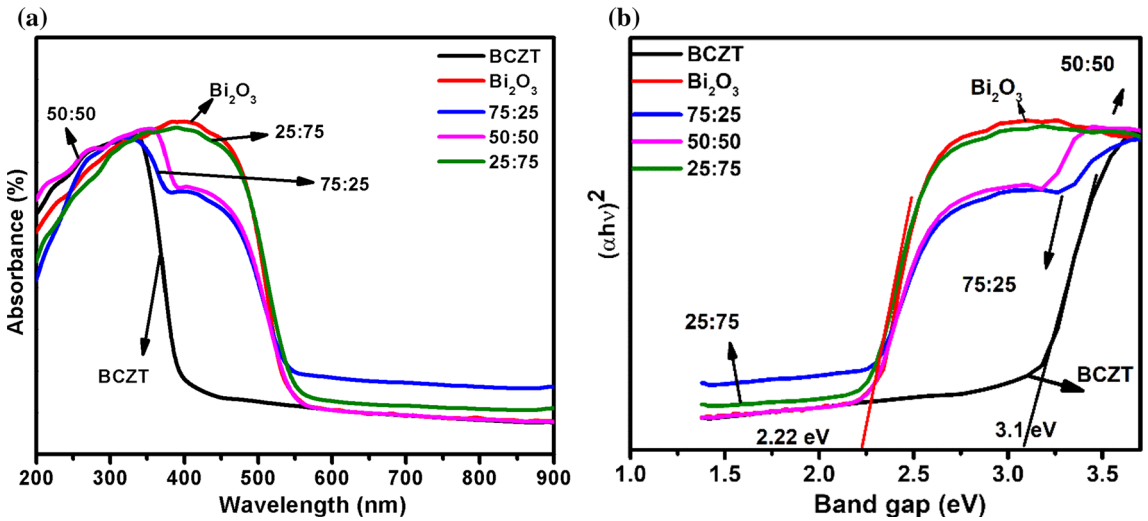

Figure 2 UV–Vis absorption spectra of BCZT, Bi_2O_3 and BCZT/Bi_2O_3 composites.

composites can play a significant role in photocatalytic degradation of RhB under visible light irradiation.

FESEM analysis of BCZT/Bi_2O_3 composites

Figure 3 shows the FESEM micrograph of BCZT, Bi_2O_3 and calcined BCZT/Bi_2O_3 composite powders. From the micrograph, it can be observed that BCZT particles are agglomerated and submicron in size, while the Bi_2O_3 consists of spherical and plate like nature. BCZT/Bi_2O_3 composite contains both irregular and spherical kind of particles. The distribution of Bi_2O_3 on the surface of BCZT was further confirmed by EDS. Figure 4 shows the EDS color mapping of the BCZT/Bi_2O_3 composite samples. From the color mapping of the images, it can be found that the concentration of Bi_2O_3 increases on the surface of BCZT with an increase in BCZT/Bi_2O_3 molar ratio.

Photoluminescence spectroscopy of BCZT/Bi_2O_3 composites

The room-temperature PL spectra of BCZT and BCZT/Bi_2O_3 composites are shown in Fig. 5. The samples are excited at 427 , nm and all the samples show green emission (525 nm). The existence of visible light emission may be due to the inherent properties of perovskites structure [27]. The green emission band observed at 525 nm is frequently caused by the electron transition from the conduction band to oxygen antisites or by donor–acceptor recombination [28]. However, for BCZT/Bi_2O_3 composites, similar emission occurs with primary peak around 525 nm. In general, a high intensity in PL is attributed to the high recombination rate of electrons and holes. Therefore, lower intensity of PL reveals lower recombination probability of charge carriers and PL analysis can be regarded as an efficient approach to study the separation efficiency of photo-generated carriers [27, 28]. Due to formation of heterojunction, PL quenching is observed in BCZT/Bi_2O_3 composites, showing that heterojunctions possess lower recombination probability of photo-generated carriers compared to that of pure BCZT. Furthermore, lowest PL intensity observed for 50:50 composite among all the samples confirms the enhancement of charge separation capability in heterostructure catalyst between BCZT and Bi_2O_3.

Photocatalytic activity of BCZT/Bi_2O_3 composites

The photocatalytic activity of as-prepared BCZT/Bi_2O_3 composites was carried out under UV and visible light irradiation with time for degradation of RhB which has a significant peak at 554 nm. Figure 6 shows the degradation of the dye for all the samples as a function of time. From Fig. 6a, b, it can be observed that BCZT, Bi_2O_3 and BCZT/Bi_2O_3 (75:25, 50:50 and 25:75) composites can degrade only 23%, 33%, 66.5%, 85% and 53% of the dye after 60 min of UV light irradiation and 14%, 66%, 75.4%, 92% and 70% of the dye after 60 min of visible light irradiation. The experiment was also performed on RhB

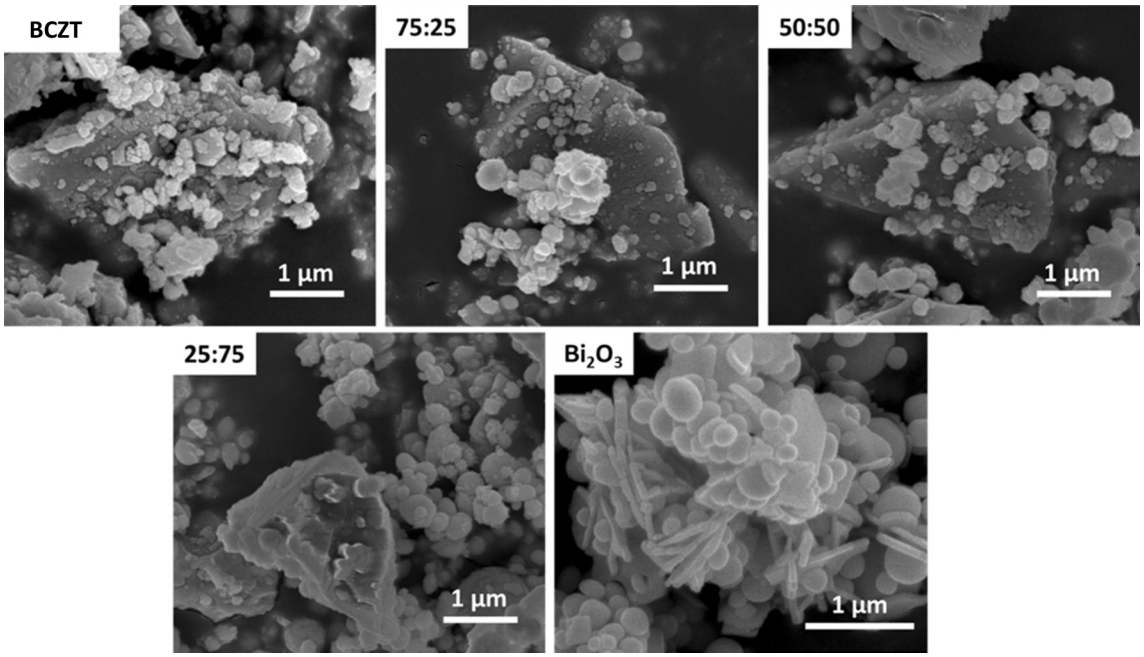

Figure 3 FESEM micrograph of pure BCZT, Bi_2O_3, and BCZT/Bi_2O_3 composites.

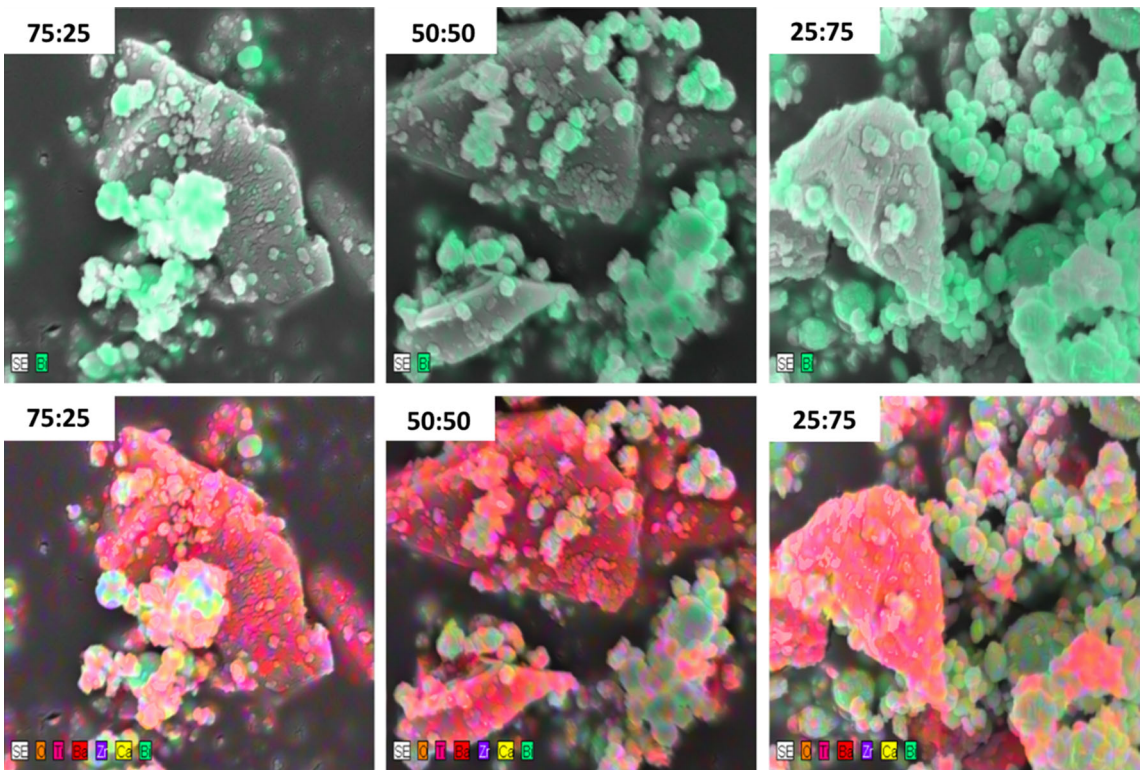

Figure 4 EDS color mapping of BCZT/Bi_2O_3 composite.

without adding any photocatalyst, and it has been observed that no degradation took place after illuminating for 1 h. It means that the degradation of dye took place only in the presence of photocatalyst. It was observed that 50:50 composite has yielded highest RhB degradation which was 3.69 and 2.5, under UV light irradiation and 6.5 and 2.5 times better than BCZT and Bi_2O_3 samples under visible

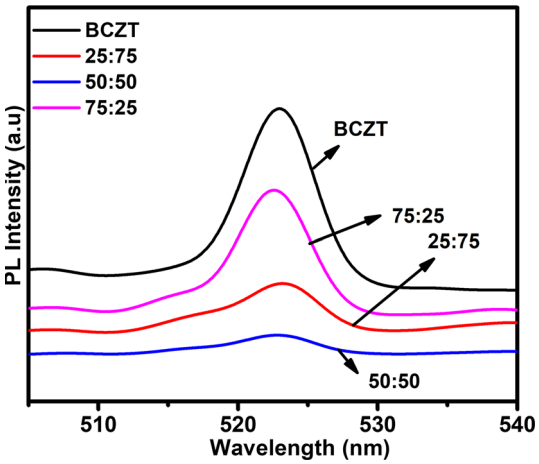

Figure 5 Photoluminescence (PL) spectra of the different photocatalysts excited at 427 nm at room temperature.

light irradiation. For comparison, the commercial P25 was also studied under similar irradiation condition and it can degrade 87% and 60% of the RhB solution in 60 min under UV and visible irradiation conditions, respectively. It is clear that the photocatalytic activity of BCZT/Bi_2O_3(50:50) is comparable to the P25 under UV irradiation but almost 50% higher than the P25 under visible light irradiation. To quantitatively analyze the reaction kinetics of RhB degradation, the experimental data in Fig. 7 could be fitted by the Langmuir–Hinshelwood model, as expressed by the following equation [29]:

$$\ln(C_o/C) = K_o t \quad (2)$$

where C_o and C are the concentrations of RhB at different irradiation times of t_o and t, respectively, and "k" is the pseudo-first-order rate constant of photodegradation (min^{-1}). From the linear fitting curves of $\ln(C_o/C)$ versus irradiation time 't' in Fig. 7a, b, the RhB degradation rate constant k was found to be 0.0044, 0.0065, 0.0187, 0.030 and 0.012 under UV light irradiation for the BCZT, Bi_2O_3 and BCZT/Bi_2O_3 (75:25, 50:50 and 25:75) composites, respectively. Under visible light irradiation, the rate constants were 0.0025, 0.0188, 0.0237, 0.0395 and 0.0204 for the BCZT, Bi_2O_3 and BCZT/Bi_2O_3 (75:25, 50:50 and 25:75) composites, respectively. Among them, the 50:50 sample exhibited the highest k value which is 6.87 and 4.64, 15.4 and 2.1 times greater than that of BCZT and Bi_2O_3 samples under UV and visible light irradiation.

We have also studied the adsorption capacity of the catalyst with time before the light was turned on. The concentration of the dye decreases very marginally with time because of the adsorption of the dye molecules on the catalyst surface. In addition, the degradation of the dye due to the adsorption is very small [1.7% for BCZT and 2.8% for BCZT/Bi_2O_3 (50:50) after 30 min] as compared to the high degradation in the presence of light. So, we have not considered the contribution of the adsorption in the calculation of the rate constant.

During synthesis of $BaTiO_3/Bi_2O_3$ composite by precipitation method, Fan et al. [19] found that with their best composition $BaTiO_3/Bi_2O_3$ (40:60) degraded RhB solution within 80 min under UV exposure whereas 4 h was required for the same under visible light exposure. Also, Ye et al. [18] reported that while synthesis of $KNbO_3/Bi_2O_3$ by solid-state method with their best composition $KNbO_3/Bi_2O_3$ (30:70)

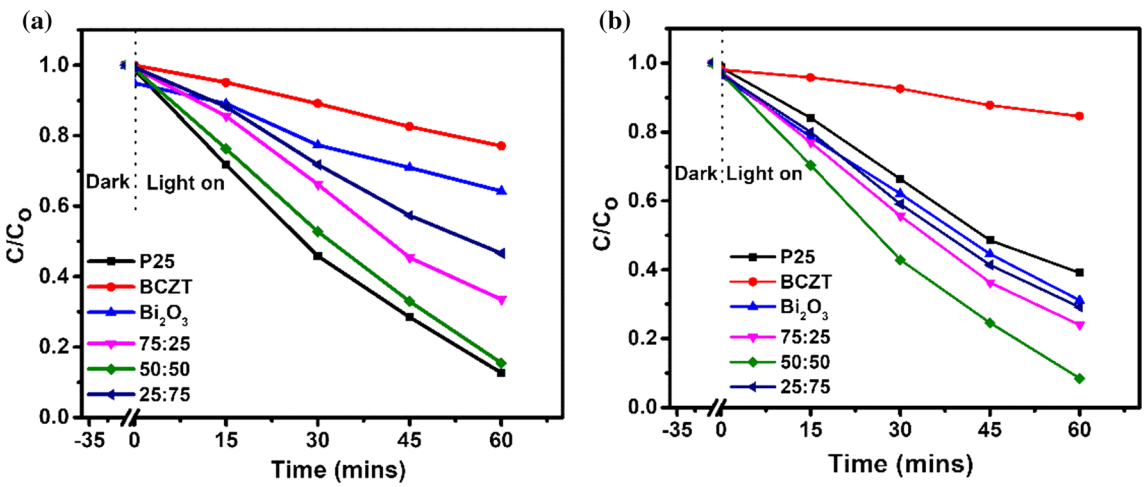

Figure 6 Change in concentration of RhB versus time under **a** UV and **b** visible light irradiation.

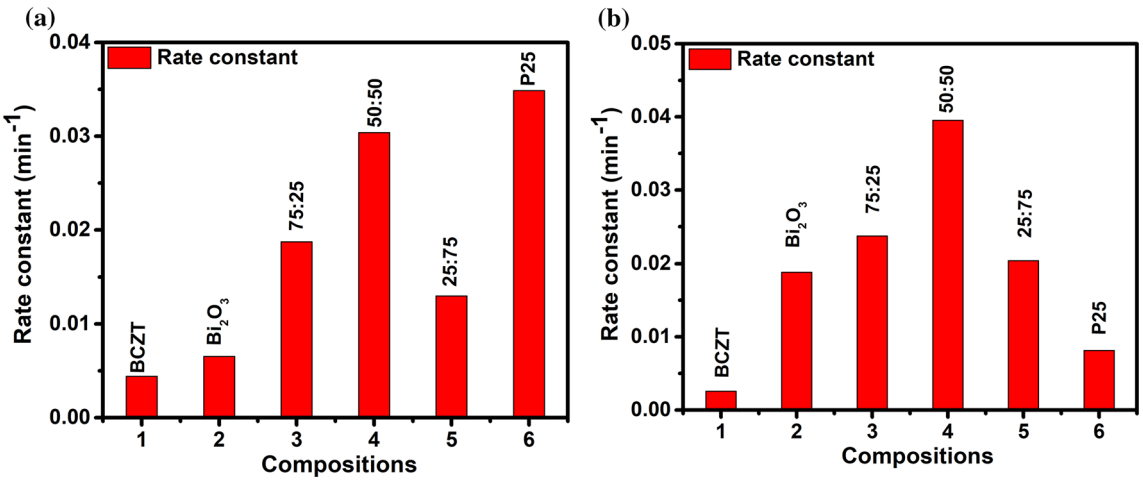

Figure 7 Rate constants of BCZT, Bi_2O_3 and BCZT/Bi_2O_3 composites under **a** UV and **b** visible light irradiation.

degraded RhB and methyl orange (MO) solution within 50 min. Their rate constant of the composite was 3.7 and 6.9 times faster than that of pure $KNbO_3$ and Bi_2O_3, respectively. In our case, 85% and 92% degradation of RhB solution happened after 60 min of UV and visible light irradiation, respectively, for 50:50 BCZT/Bi_2O_3 composition which is much better than the previous results.

The enhancement of photocatalytic activity for composite samples can mainly be attributed to the enhanced absorption in visible region and secondly due to the electric field-assisted charge transfer at the heterojunction interfaces between BCZT and Bi_2O_3 with matching band potentials, which consequently prevents the recombination of electrons and holes. The conduction band (CB) and valence band (VB) potentials of BCZT and Bi_2O_3 are calculated by using the following formulas [29]

$$E_{VB} = \chi - E^e + 0.5E_g \quad (3)$$

$$E_{CB} = E_{VB} - E_g \quad (4)$$

where E_{VB} is the valence band potentials of a semiconductor, χ is the electronegativity of a semiconductor which is the geometric mean of electronegativity of constituent atoms (Ba, Ti, Zr, Ca, Bi and O) and E^e is the energy of free electron on hydrogen scale (4.5 eV VS NHE). By using the above formula, the CB and VB potentials of BCZT are found to be − 0.94 and 2.16 eV and for Bi_2O_3 the values are found to be 0.63 and 2.83 eV, respectively. Under light irradiation, electrons present in the CB of Bi_2O_3 (0.63 eV) are more positive than the potential of O_2/$^*O_2^-$ (− 0.33 eV); therefore, the e^- on the conduction band of Bi_2O_3 cannot reduce the adsorbed O_2 into $^*O_2^-$. Holes present in the VB of BCZT (2.16 eV) (considering the over potentials 0.2 eV) cannot oxidize H_2O and OH^- into OH^* since the VB potential of BCZT was less than OH^*/H_2O (2.27 eV) and OH^*/OH^- (1.99 eV) potentials. So, in the present case photocatalytic degradation does not happen by a simple band-to-band transfer of electrons and holes. Here, a direct Z-scheme mechanism comes into play because the CB potential of BCZT has strong reduction ability and holes in the VB of Bi_2O_3 have strong oxidation ability [30]. When tight bonding occurs between BCZT and Bi_2O_3 due to their matching band potentials, band bending occurs at the interface which induces an inbuilt electric field across the interfaces. Thus, the internal electric field pushes the electrons and holes in the opposite direction, leading to a spatial separation of electrons and holes on different sides of heterojunction. The charge transfer mechanism is shown in Fig. 8.

Effect of pH on RhB degradation

The pH value has an important influence on the photodegradation of dye because it can influence the surface charge properties of a photocatalyst and ionic species in the solution [31–33]. Figure 9 displays the photocatalytic degradation of BCZT/Bi_2O_3 (50:50) composite as a function of pH. Initial pH of the RhB solution was ∼ 5. The result shows that when the pH of the RhB solution was reduced to 3, the degradation efficiency increased to 90% in 45 min of visible light irradiation. With a further decrease in pH to 1, complete mineralization can be observed in 30 min.

The higher degradation in low pH condition (pH < 5) occurs due to the electrostatic attraction between the negative charge of the BCZT/Bi_2O_3 catalyst and the positive charge of RhB [31, 32]. Moreover, at high initial pH values of 9 and 11, the percentage degradation was 54 and 23, respectively, which can be explained by the deprotonation of the carboxyl group of RhB and the transformation of the cationic form of RhB into zwitterionic form [31, 32].

Identification of active species in photocatalytic reactions

To understand the role of active species on RhB degradation, photocatalytic experiments were carried out under visible light irradiation with different scavengers. To do this, 1 mM of benzoquinone (as O_2^- scavenger), 1 mM of IPA (isopropyl alcohol) (as.OH scavenger) and 1 mM of oxalic acid (as h^+ scavenger) were added separately to RhB solution. Figure 10a shows the degradation of RhB for 50:50 BCZT/Bi_2O_3 sample with and without addition of scavengers as a function of irradiation time. From Fig. 10a, it can be observed that 50:50 BCZT/Bi_2O_3 can degrade 92% of the dye after 60 min of visible light irradiation. When benzoquinone was added into the system, only 60% of the dye was degraded. Degradation of RhB was also suppressed (38%) when IPA was added into the system. When oxalic acid was added into the system, 30% of the RhB was degraded in 60 min of photocatalytic experiment. RhB degradation was highly quenched when oxalic acid was added. Based on the above observation, it may be possible that O_2^-, OH^* and h^+ could play an important role in photocatalytic

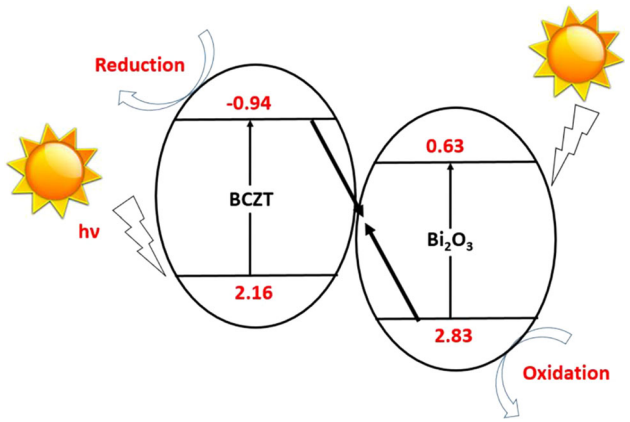

Figure 8 Charge transfer mechanism in BCZT/Bi_2O_3 composites.

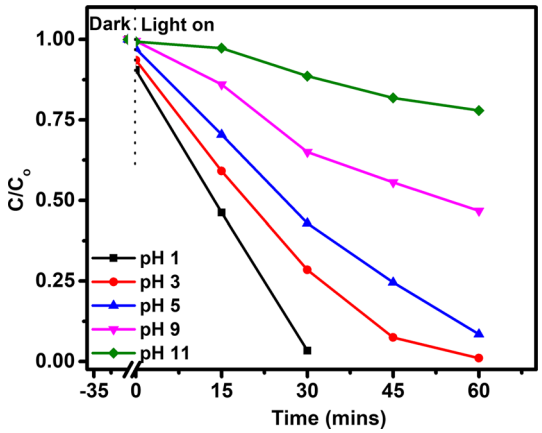

Figure 9 Photocatalytic degradation of BCZT/Bi_2O_3 (50:50) composite as a function of pH.

degradation of RhB under visible light. Based on the above results, the probable mechanism for the degradation of RhB by 50:50 BCZT/Bi_2O_3 composite is shown in Fig. 10b. Finally, the reusability of the photocatalyst was also examined and showed ~ 5% decrease in efficiency for RhB degradation under visible light irradiation, after five cycles of reuse as shown in Fig. 10c.

Conclusions

BCZT/Bi_2O_3 composite was successfully prepared by solid-state method at 500 °C to form a composite without any intermediate phase. Absorption edge shifts toward visible region of light for composites samples. FESEM micrographs show uniform distribution of BCZT and Bi_2O_3 in the composite powder. BCZT/Bi_2O_3 composite sample shows better photocatalytic activity under both UV and visible light irradiation than that of the pure BCZT and Bi_2O_3. BCZT/Bi_2O_3 (50:50) composite sample can degrade 92% of the RhB solution in 60 min under visible light irradiation. However, commercial P25 can degrade 60% of the RhB solution in 60 min under similar irradiation condition. The pH value has an important influence on the adsorption and the photocatalytic degradation of RhB upon BCZT/Bi_2O_3 composite. A large adsorption and degradation of the dye is observed at relatively low pH values (pH < 5). The photocatalytic degradation of RhB under visible light irradiation in the presence of different scavengers confirms that hole (h^+) and superoxide radicals (O_2^-) were found to be the dominant active species for

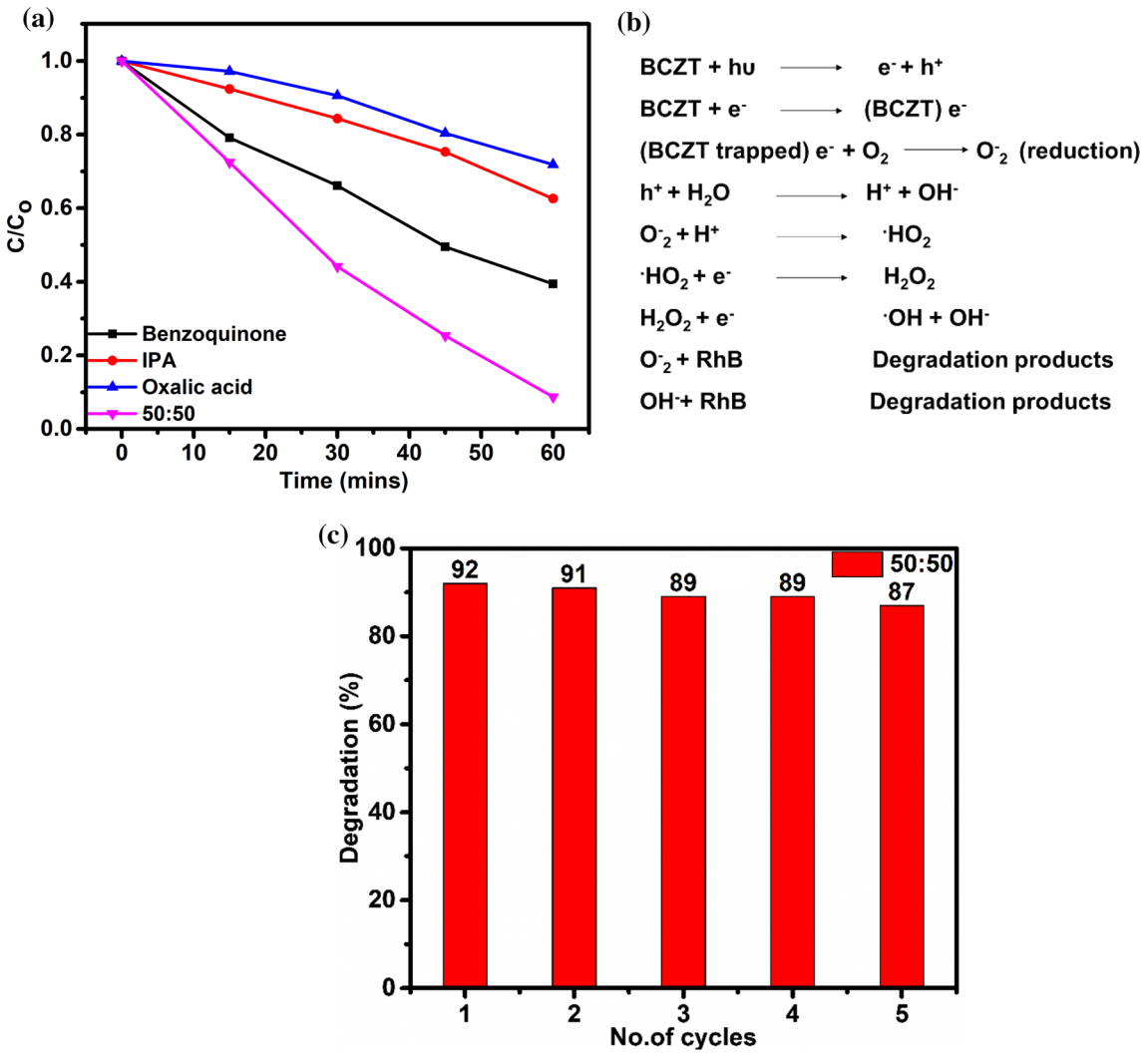

Figure 10 **a** Change in concentration of RhB versus time under visible light irradiation with and without addition of scavengers, **b** electron and hole transfer mechanism in 50:50 BCZT/Bi_2O_3 composite, **c** cyclic stability of 50:50 BCZT/Bi_2O_3 composite as a visible light photocatalyst for five cycles.

BCZT/Bi_2O_3 composite sample. In this system, the electrons present in the conduction band of Bi_2O_3 cannot reduce the adsorbed O_2 into $^*O_2^-$ and holes present in the valence band of BCZT cannot oxidize H_2O and OH^- into OH^*. So, in the present case photocatalytic degradation does not happen by a simple band-to-band transfer of electrons and holes. In BCZT/Bi_2O_3 composites, the Z-scheme principle of photocatalyst is confirmed owing to its stronger oxidation and reduction capability.

Acknowledgements

We are thankful to the Director, NIT Rourkela, Odisha, India, for providing experimental facilities.

Compliance with ethical standards

Conflict of interest The authors declare no conflict of interest.

References

[1] Gaya UI, Abdullah AH (2008) Heterogeneous photocatalytic degradation of organic contaminants over titanium dioxide: a

review of fundamentals, progress and problems. J Photochem Photobiol C Photochem Rev 9:1–12

[2] Boppella R, Anjaneyulu K, Basak P, Manorama SV (2013) Facile synthesis of face oriented ZnO crystals: tunable polar facets and shape induced enhanced photocatalytic performance. J Phys Chem C 117:4597–4605

[3] Shakir I, Shahid M, Kang DJ (2013) Highly functional SnO_2 coated PZT core-shell heterostructures as a visible light photocatalyst for efficient water remediation. Chem Eng J 225:650–655

[4] Wang H, Zhang L, Chen Z et al (2014) Semiconductor heterojunction photocatalysts: design, construction, and photocatalytic performances. Chem Soc Rev 43:5234–5244

[5] Wu Q, Li D, Wu L et al (2006) Unprecedented application of lead zirconate titanate in degradation of Rhodamine B under visible light irradiation. J Mater Chem 16:1116–1117

[6] Huang H, Li D, Lin Q et al (2009) Efficient photocatalytic activity of PZT/TiO_2 heterojunction under visible light irradiation. J Phys Chem C 113:14264–14269

[7] Cui Y, Briscoe J, Dunn S (2013) Effect of ferroelectricity on solar-light-driven photocatalytic activity of $BaTiO_3$—Influence on the carrier separation and stern layer formation. Chem Mater 25:4215–4223

[8] Xiong X, Li S, Tian R et al (2015) Formation and photocatalytic activity of $BaTiO_3$ nanocubes via hydrothermal process. J Nanomater 2015:1–6

[9] Kappadan S, Woldu T, Thomas S, Kalarikkal N (2016) Materials science in semiconductor processing tetragonal $BaTiO_3$ nanoparticles: an efficient photocatalyst for the degradation of organic pollutants. Mater Sci Semicond Process 51:42–47

[10] Kaya C, Kalem V, Teber S (2018) Photocatalytic activity and dielectric properties of hydrothermally derived tetragonal $BaTiO_3$ nanoparticles using TiO_2 nano fibers. J Alloys Compd 765:82–91

[11] Fu Q, Wang X, Li C et al (2016) Enhanced photocatalytic activity on polarized ferroelectric $KNbO_3$. RSC Adv 6:108883–108887

[12] Tonda S, Santosh Kumar OA, Shanker V (2014) Synthesis of Cr and La-codoped SrTiO 3 nanoparticles for enhanced photocatalytic performance under sunlight irradiation. Phys Chem Chem Phys 16:23819–23828

[13] Yang SY, Seidel J, Byrnes SJ et al (2010) Above-bandgap voltages from ferroelectric photovoltaic devices. Nat Nanotechnol 5:143–147

[14] Morris MR, Pendlebury SR, Hong J et al (2016) Effect of internal electric fields on charge carrier dynamics in a ferroelectric material for solar energy conversion. Adv Mater 28:7123–7128

[15] Li L, Salvador PA, Rohrer GS (2014) Photocatalysts with internal electric fields. Nanoscale 6:24–42

[16] Zhao X, Liu H, Qu J (2011) Photoelectrocatalytic degradation of organic contaminants at Bi_2O_3/TiO_2 nanotube array electrode. Appl Surf Sci 257:4621–4624

[17] Lin X, Xing J, Wang W et al (2007) Photocatalytic activities of heterojunction semiconductors $Bi_2O_3/BaTiO_3$: a strategy for the design of efficient combined photocatalysts. J Phys Chem C 111:18288–18293

[18] Ye X, Zhao S, Meng S et al (2017) Remarkable enhancement of photocatalytic performance via constructing a novel Z-scheme $KNbO_3/Bi_2O_3$ hybrid material. Mater Res Bull 94:352–360

[19] Fan H, Li H, Liu B et al (2012) Photoinduced charge transfer properties and photocatalytic activity in $Bi_2O_3/BaTiO_3$ composite photocatalyst. ACS Appl Mater Interfaces 4:4853–4857

[20] Chu S, Kong F, Wu G et al (2011) Architecture of $Cu_2O@TiO_2$ core-shell heterojunction and photodegradation for 4-nitrophenol under simulated sunlight irradiation. Mater Chem Phys 129:1184–1188

[21] Zhou W, Liu H, Wang J et al (2010) Ag_2O/TiO_2 nanobelts heterostructure with enhanced ultraviolet and visible photocatalytic activity. ACS Appl Mater Interfaces 2:2385–2392

[22] Cui Y, Briscoe J, Wang Y et al (2017) Enhanced photocatalytic activity of heterostructured ferroelectric $BaTiO_3/\alpha$-Fe_2O_3 and the significance of interface morphology control. ACS Appl Mater Interfaces 9:24518–24526

[23] Jiang HY, Cheng K, Lin J (2012) Crystalline metallic Au nanoparticle-loaded α-Bi_2O_3 microrods for improved photocatalysis. Phys Chem Chem Phys 14:12114–12121

[24] Liu W, Ren X (2009) Large piezoelectric effect in Pb-free ceramics. Phys Rev Lett 103:1–4

[25] Abhinay S, Mazumder R, Seal A, Sen A (2016) Tape casting and electrical characterization of $0.5Ba(Zr_{0.2}Ti_{0.8})O_3$–$0.5(Ba_{0.7}Ca_{0.3})TiO_3$ (BZT–0.5BCT) piezoelectric substrate. J Eur Ceram Soc 36:3125–3137

[26] Adhikari P, Mazumder R, Abhinay S (2016) Electrical and mechanical properties of MgO added $0.5Ba(Zr_{0.2}Ti_{0.8})O_3$–$0.5(Ba_{0.7}Ca_{0.3})TiO_3$ (BZT–0.5BCT) composite ceramics. J Electroceram 37:127–136

[27] Raja S, Ramesh Babu R, Ramamurthi K, Moorthy Babu S (2018) Room temperature ferromagnetic behavior, linear and nonlinear optical properties of $KNbO_3$ microrods. Ceram Int 44:3297–3306

[28] Andrade GRS, Nascimento CC, Silva Júnior EC et al (2017) ZnO/Au nanocatalysts for enhanced decolorization of an azo dye under solar, UV-A and dark conditions. J Alloys Compd 710:557–566

[29] Wei K, Wang B, Hu J et al (2019) Photocatalytic properties of a new Z-scheme system $BaTiO_3$/In2S3 with a core-shell structure. RSC Adv 9:11377–11384

[30] Xu Q, Zhang L, Yu J et al (2018) Direct Z-scheme photocatalysts: principles, synthesis, and applications. Mater Today 21:1042–1063

[31] You-Ji L, Wei C (2011) Photocatalytic degradation of Rhodamine B using nanocrystalline TiO_2-zeolite surface composite catalysts: effects of photocatalytic condition on degradation efficiency. Catal Sci Technol 1:802–809

[32] Tabit R, Amadine O, Essamlali Y et al (2018) Magnetic $CoFe_2O_4$ nanoparticles supported on graphene oxide ($CoFe_2O_4$/GO) with high catalytic activity for peroxymonosulfate activation and degradation of rhodamine B. RSC Adv 8:1351–1360

[33] Natarajan TS, Thomas M, Natarajan K et al (2011) Study on UV-LED/TiO_2 process for degradation of Rhodamine B dye. Chem Eng J 169:126–134